Journal of Power Sources 185 (2008) 1354–1358

Contents lists available at ScienceDirect

Journal of Power Sources

journal homepage: www.elsevier.com/locate/jpowsour

Short communication

The effect of heating rate on the reversible hydrogen storage based on reactions of Li_3AlH_6 with $LiNH_2$

Jun Lu [a], Zhigang Zak Fang [a,*], Young Joon Choi [a], Hong Yong Sohn [a], Chul Kim [b], Robert C. Bowman Jr. [c], Son-Jong Hwang [b]

[a] Department of Metallurgical Engineering, University of Utah, 135 South 1460 East Room 412, Salt Lake City, UT 84112, USA
[b] The Division of Chemistry and Chemical Engineering, California Institute of Technology, Pasadena, CA 91125, USA
[c] Jet Propulsion Laboratory, California Institute of Technology, Pasadena, CA 91109, USA

ARTICLE INFO

Article history:
Received 15 May 2008
Received in revised form 10 July 2008
Accepted 10 July 2008
Available online 25 July 2008

Keywords:
Hydrogenation
Dehydrogenation
Heating rate
Alanate
Amide

ABSTRACT

Reversible dehydrogenation and hydrogenation reactions have been reported for a number of reactions based on lithium alanate and lithium amide materials. The dehydrogenation and hydrogenation reactions involving these materials are, however, usually very complex. Significant discrepancies exist among different studies published in literature. Understanding the reaction mechanism and the dependence of the reaction pathway on material preparation processes and processing parameters is critical. In this paper, the hydrogenation reactions of the mixture of $3Li_2NH/Al/4$ wt%$TiCl_3$ were investigated as a function of the heating rate. The hydrogenated products were characterized by means of TGA, XRD and solid-state NMR. These new results showed that the re-formation of Li_3AlH_6 depends strongly on the heating rate during the hydrogenation process. The dehydrogenation and rehydrogenation reaction pathways and possible mechanisms of the combined system are, however, still under investigation.

1. Introduction

In recent years, lithium aluminum hydrides ($LiAlH_4$ and Li_3AlH_6) have received a great deal of attention as hydrogen storage materials because of their lightweight and high inherent storage capacities [1–11]. However, complete reversible dehydrogenation and hydrogenation of lithium aluminum hydrides are not possible under moderate conditions with the temperature lower than 300 °C and hydrogen pressure lower than 200 bar [12]. Several recent studies demonstrated a different approach for extracting hydrogen from lithium alanates by subjecting them to reactions with other chemical compounds, such as amides, that destabilize the alanates and lower the activation energy of dehydrogenation [13,14]. For example, the present authors [14] found that the reversible hydrogen storage with approximately 7.0 wt% capacity is feasible under 300 °C using a combined alanate/amide system according to the following reaction:

$$Li_3AlH_6 + 3LiNH_2 \leftrightarrow Al + 3Li_2NH + \frac{9}{2}H_2 \quad (1)$$

However, the re-formation of Li_3AlH_6 by the reverse reaction of Eq. (1) is still a debatable subject. The analysis of several other published studies of similar reaction systems revealed significantly different results. For example, Kojima et al. [15] investigated the mixture of $Li_3AlH_6/2LiNH_2$ for reversible hydrogen storage applications. They found that Li_3AlN_2 and/or AlN formed during the hydrogenation process. Xiong et al. [16] also found that Li_3AlN_2 formed in the dehydrogenation of the mixture of $LiAlH_4/2LiNH_2$.

Understanding the discrepancies shown by different studies of similar systems needs to be better rationalized with systematic experimental demonstrations. It is hypothesized that the reaction pathways and products are affected by molar ratios of the reactants, experimental parameters such as temperature, heating rate, cooling rate, and material preparation techniques such as ball milling processes. These different experimental factors could affect the reaction mechanisms during the hydrogen absorption/desorption process.

In this work, the effect of the heating rate on the hydrogenation of $3Li_2NH + Al$, i.e. the reverse reaction of Eq. (1), was studied. As will become clear through the results presented below, the re-formation of Li_3AlH_6 by Eq. (1) depends strongly on the heating rate during the hydrogenation process. The discovery of the effect of heating rate yields a strong clue to understanding the dehydrogenation and rehydrogenation reaction pathways and mechanisms.

* Corresponding author. Tel.: +1 801 581 8128; fax: +1 801 581 4937.
E-mail address: zak.fang@utah.edu (Z.Z. Fang).

0378-7753/$ – see front matter © 2008 Elsevier B.V. All rights reserved.
doi:10.1016/j.jpowsour.2008.07.040

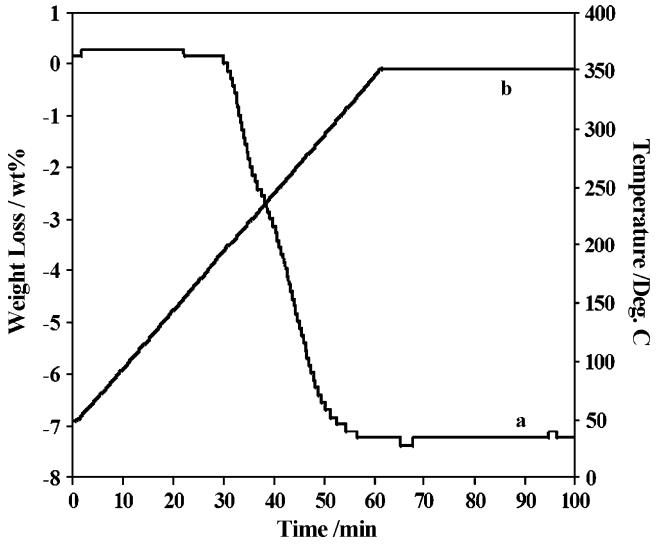

Fig. 1. TGA curves for the pre-milled $3LiNH_2/Li_3AlH_6/4\,wt\%TiCl_3$. Curve (a) shows the hydrogen release under argon. Curve (b) shows the temperature profile.

2. Experimental

The starting materials, Li_3AlH_6, $LiNH_2$ and $TiCl_3$, were purchased from GFS and Aldrich Chemical, respectively, and used as received without any further purification. They were stored and handled in an argon-filled glove box to prevent the raw materials and samples from oxidation and/or hydroxide formation. Reactant mixtures were prepared using mechanical milling. Approximately 2.0 g mixtures with a molar ratio of Li_3AlH_6:$LiNH_2$ = 1:3 were milled in a jar-roll mill under argon atmosphere with a ball to powder ratio of 35:1 by weight. The milling time was varied from 12 to 48 h and at a milling speed of 120 rpm. $TiCl_3$ was added at 4 wt% as a catalyst for the rehydrogenation reaction [1].

The gas release properties of the mixtures were determined by a thermogravimetric analyzer (TGA, Shimadzu TGA50) by heating the sample up to 300 °C at a heating rate of 5 °C min^{-1}. This equipment was specially designed and built to be used inside an argon-filled glove box equipped with a gas purification system, which permitted performing TGA without exposing the sample to air.

The starting mixture for the current study, $3Li_2NH/Al/4\,wt\%TiCl_3$, was prepared by heating the pre-milled mixture of $3LiNH_2/Li_3AlH_6/4\,wt\%TiCl_3$ to 300 °C. Fig. 1 shows the TGA result of the $Li_3AlH_6/3LiNH_2/4\,wt\%TiCl_3$ after ball milling treatment. Each reaction step is identified by the changes of the rate of the weight loss. It can be seen that a total of 7.1 wt% of hydrogen was released within the examined temperature range. The desorption process consists of two steps. According to our previous results [13], these two weight-loss steps can be best described by the following reactions:

$$Li_3AlH_6 \rightarrow 3LiH + Al + \tfrac{3}{2}H_2 \quad (2)$$

$$LiH + LiNH_2 \rightarrow Li_2NH + H_2 \quad (3)$$

The dehydrogenated products are confirmed to be Al and Li_2NH by XRD, FT-IR and solid-state NMR results (not shown here), which is also in agreement with our previous results [13]. The dehydrogenated samples were then rehydrogenated in a custom-made autoclave. For consistency, the samples for all the rehydrogenation experiments hereafter used fresh portion of the dehydrogenated samples from the same batch, as described above.

The hydrogenation properties of the mixture ($3Li_2NH/Al/4\,wt\%TiCl_3$) were evaluated by using a custom-made autoclave with a hydrogen pressure limit of 344 bar and a reaction temperature of up to 500 °C. Specifically, rehydrogenation was conducted by heating about 500 mg of the mixture to 300 °C with a series of heating rates (1, 2, 5, and 10 °C min^{-1}) and holding it at 300 °C for 10 h under 172 bar of hydrogen pressure.

The identification of the reactants and products before and after the thermogravimetric analysis was carried out using a Siemens D5000 model X-ray diffractometer with Ni-filtered Cu Kα radiation (λ = 1.5406 Å). Each sample for XRD analysis was mounted on a glass slide and covered with a Kapton® tape as a protective film in the glove box. A scanning rate of 0.02 ° s^{-1} was applied to record the patterns in the 2θ range between 10° and 90°. It should be noted that the amorphous-like broad peak around $20°/2\theta$ is background signal from the Kapton® tape that was used to cover the powders.

Multinuclear solid-state MAS NMR spectra were acquired using a Bruker Avance 500 MHz spectrometer with a wide bore 11.7 T magnet and employing a Bruker 4 mm CPMAS probe. The spectral frequencies were 500.23, 130.35, 73.61 MHz for ^{1}H, ^{27}Al, ^{6}Li nuclei, respectively, and NMR shifts were reported in parts per million (ppm) with respect to external references: tetramethylsilane (TMS) for ^{1}H, 1.0 molar LiCl aqueous solution for ^{6}Li, and 1.0 molar $Al(NO_3)_3$ aqueous solution for ^{27}Al nuclei. In an argon atmosphere glove box, the powder samples were packed into 4 mm ZrO_2 rotors after minimal additional grinding and were sealed with a tight fitting kel-F cap. The NMR samples were stored under argon until inserted into the spectrometer probe where sample spinning was performed using dry nitrogen gas. For quantitative analyses, ^{27}Al MAS NMR spectra were obtained at sample spinning rates of 12–14 kHz and using a short (0.3 μs) single pulse (<π/18) with the application of a strong ^{1}H decoupling pulse of the two-pulse phase modulation (TPPM) scheme [17].

3. Results and discussions

In order to investigate the effect of the heating rate during hydrogenation, the mixtures of $3Li_2NH/Al/4\,wt\%TiCl_3$ were heated from the room temperature to 300 °C with different heating rates from 1 to 10 °C min^{-1} under 172 bar hydrogen pressure then held at 300 °C for 10 h. These hydrogenated samples were subsequently analyzed using TGA, XRD and solid-state NMR. For simplicity, the samples are designated as Samples 1, 2, 3 and 4 for the heating rates of 1, 2, 5 and 10 °C min^{-1}, respectively.

3.1. TGA analysis

Fig. 2A and B shows TGA profiles of the Sample 1 and 2, the hydrogenated mixtures of $3Li_2NH/Al/4\,wt\%TiCl_3$ employing heating rates of 1 and 2 °C min^{-1}, respectively. The profiles at both cases show that the samples took up hydrogen amounting to about 4 wt% of the hydrogenated products. The dehydrogenation reaction of these hydrogenated samples appears to be a one-step process rather than a two-step process, of which example is shown in Fig. 1 for the initial mixture according to Eqs. (2) and (3). Fig. 2A and B also shows that the hydrogen contents of the samples prepared using the heating rates of 1 and 2 °C min^{-1} are less than that of the initial mixture.

However, the situation changed dramatically when the heating rate is increased. Shown in Fig. 2C and D are the TGA profiles for the hydrogenated samples prepared using the heating rates of 5 and 10 °C min^{-1}, respectively. Under these conditions, TGA weight loss curves show that the samples took up approximately 6.8 wt% of hydrogen, calculated on the basis of the hydrogenated products, which is close to that of the initial mixture. Moreover, the dehydrogenation reaction of these hydrogenated samples appears to be

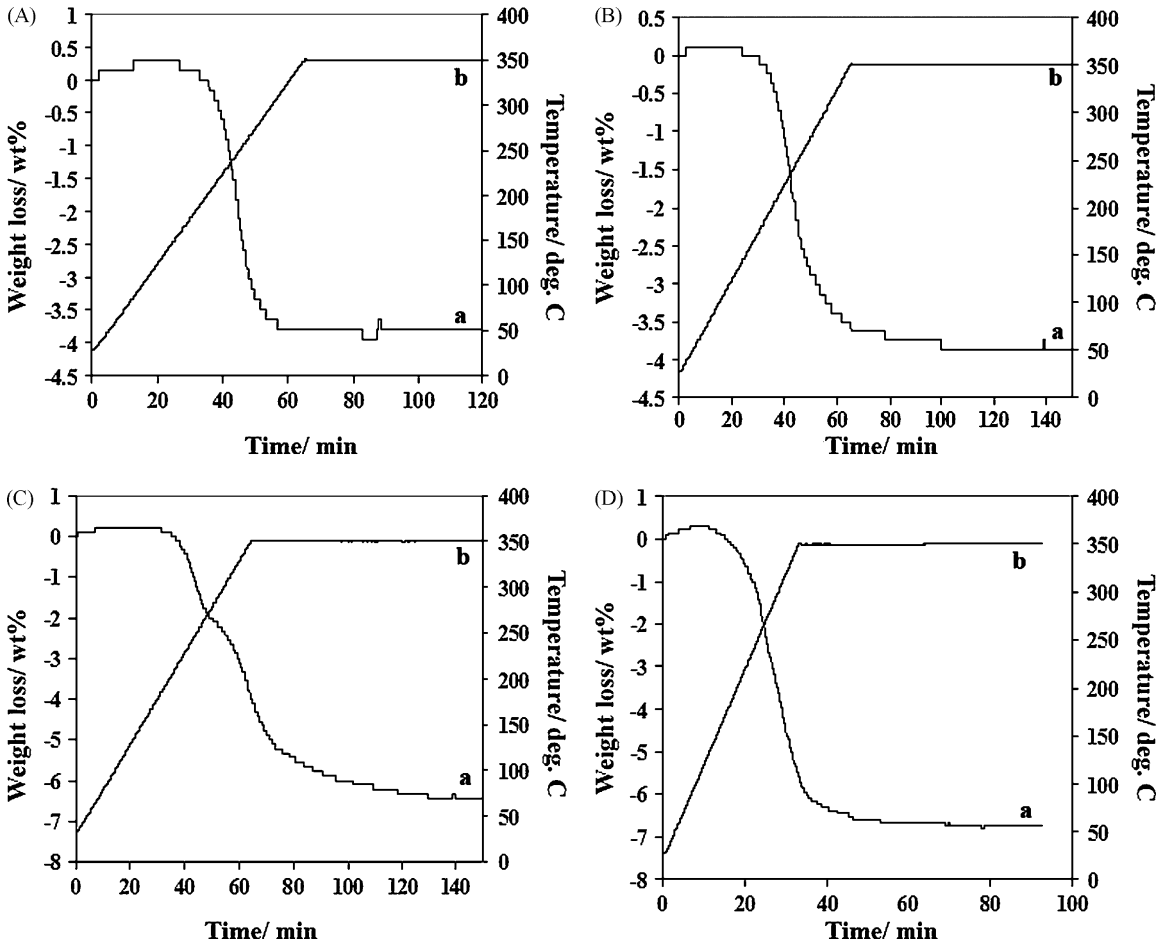

Fig. 2. TGA curves for $3Li_2NH/Al/4\,wt\%TiCl_3$ after hydrogenation at 300 °C under 172 bar hydrogen pressure under the different heating rates: (A) 1 °C min^{-1}; (B) 2 °C min^{-1}; (C) 5 °C min^{-1} and (D) 10 °C min^{-1}. Curve a shows the hydrogen release under argon. Curve b shows the temperature profile.

a two-step process in the TGA curves, similar to that of the initial mixture as shown in Fig. 1. The weight-loss values of the hydrogenated $3Li_2NH/Al/4\,wt\%TiCl_3$ prepared using the various heating rates are further compared in Table 1. The comparison suggests that the hydrogenation pathway of the mixture of $3Li_2NH/Al/4\,wt\%TiCl_3$ is significantly affected by the heating rate that was used in the process of reaching to the same designated reaction temperature (300 °C).

The underlying assumption of the above TGA analysis is that the weight gain of the samples after processing is due to hydrogen uptake. Unambiguous proof of the hydrogenation reactions, however, requires further studies.

3.2. XRD characterizations of the hydrogenated $3Li_2NH/Al/4\,wt\%TiCl_3$

X-ray powder diffraction was used to analyze the samples after the series of hydrogenation treatments. Crystalline phases are identified by comparing the experimental data with JCPDS files. To identify chemical species that are present in the hydrogenated samples, the XRD patterns for selected pure materials, which were expected to be parts of the rehydrogenation products, are also shown as vertical bars in Fig. 3 for comparison. Fig. 3A–D shows the XRD patterns of the hydrogenated samples (i.e., Samples 1–4) with the heating rates of 1, 2, 5, and 10 °C min^{-1}, respectively. The peaks marked with "1" are attributed to $LiNH_2$ phase and those marked with "3" are attributed to Al, LiH, or possibly AlN. The presence of monoclinic Li_3AlH_6 can be identified by the characteristic double peak at 2θ values of approximately 22° as was marked with "2". It is clear from Fig. 3 that the formation of the Li_3AlH_6 phase is influenced by the heating rates during the hydrogenation process. Sustaining of the Li_3AlH_6 phase was found to occur only when the heating rate was greater than 5 °C min^{-1}, indicating that the formation of Li_3AlH_6 is process dependent. At slower rates, the formation of Li_3AlH_6 is either thermodynamically unfavorable or kinetically limited. It should be noted, however, other phases including $LiNH_2$ and LiH did form during the process at slower heating rates. The XRD results are also summarized in Table 1.

Table 1
Phases detected in several Li–Al–N–H samples from XRD, and NMR measurements

Sample	Heating rates (°C min^{-1})	TGA weight loss (wt%)	Characteristic XRD peaks for Li_3AlH_6 at around 22°	NMR
1	1	3.9	No	$LiNH_2$, LiH, Al, and AlN
2	2	4.0	No	$LiNH_2$, LiH, Al, and AlN
3	5	6.8	Yes	$LiNH_2$, Li_3AlH_6, Al(minor), and Al_2O_3(minor)
4	10	6.9	Yes	$LiNH_2$, Li_3AlH_6, Al(minor), and Al_2O_3(minor)

The starting mixture was $3Li_2NH/Al/4\,wt\%TiCl_3$, and it was hydrogenated at 300 °C and 172 bar of hydrogen pressure under different heating rates.

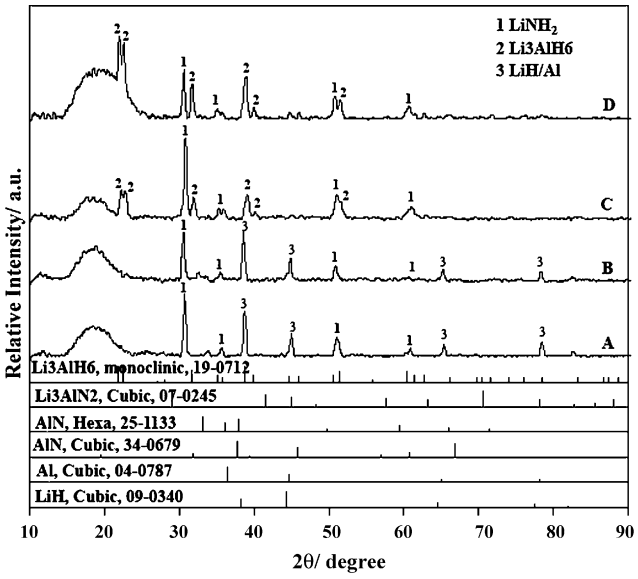

Fig. 3. XRD patterns of $3Li_2NH/Al/4$ wt%$TiCl_3$ after hydrogenation at 300 °C under 172 bar hydrogen pressure under the different heating rates: (A) 1 °C min^{-1}; (B) 2 °C min^{-1}; (C) 5 °C min^{-1} and (D) 10 °C min^{-1}. The amorphous-like broad peak is from the thin plastic films that were used to cover the powders.

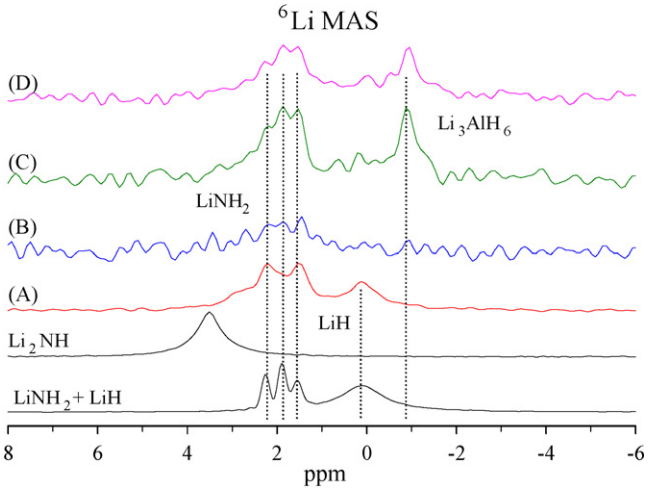

Fig. 5. ^6Li MAS NMR spectra of $3Li_2NH/Al/4$ wt%$TiCl_3$ after hydrogenation at 300 °C under 172 bar hydrogen pressure under the different heating rates: (A) 1 °C min^{-1}; (B) 2 °C min^{-1}; (C) 5 °C min^{-1} and (D) 10 °C min^{-1}. The ^6Li MAS NMR spectra of pure Li_2NH, mixture of $LiNH_2$ and LiH are provided for references (see text).

Based on the TGA and XRD results described above, however, it is still difficult to determine the reaction products that formed when the slower heating rates were used. Specifically, it is not clear if there were any nitrides formed as indicated by other references [15,16]. The presence of different phases in the rehydrogenated samples, however, can not be identified solely by using XRD, because the main peaks of some compounds overlap with each other, such as $LiNH_2$ and Li_2NH, or Al and AlN. Solid-state NMR is therefore used to analyze the reaction products as discussed below.

3.3. NMR characterizations of the hydrogenated samples

Fig. 4 shows the ^{27}Al MAS NMR spectra for the same samples whose parts were used in the TGA and XRD analyses presented above. The chemical species identified by ^{27}Al NMR are also found to be associated with the different heating rates during the hydrogenation process. The Samples 1 and 2, rates of 1 and 2 °C min^{-1}, respectively, contain aluminum metal (Al_M) in large quantity as displayed by a strong peak at around 1640 ppm in ^{27}Al NMR spectra. The result again allows us to conclude that the conversion from Al_M to Li_3AlH_6 did not occur under the slower heating rates. It is noteworthy that a very small amount of the Li_3AlH_6 phase is detected in the Sample 2. The peak at ~114 ppm observed for Samples 1 and 2, in Fig. 4A and B, respectively, might indicate the formation of aluminum nitride [18] or other nitride species such as Li_3AlN_2 as reported by Xiong et al in their recent studies of Li–Al–N–H system [16]. The peak was found not to be observed in $^{27}Al\{^1H\}$ CPMAS NMR experiments, supporting the assignment with aluminum species without bearing Al–H bonds. To determine accurately the origin of the 114 ppm peak, however, further NMR studies are planned on the specimens that are prepared to reveal the details of the evolution of the reaction process as functions of both temperature and time.

The population ratio among aluminum species that have been estimated by integrating NMR peaks was Al_M:AlN = 37:63 for Sample 1 and Al_M:AlN:Li_3AlH_6 = 41:56:3 for Sample 2. Efficient conversion from Al_M to hexahydroaluminate (AlH_6^{3-}) in Samples 3 and 4, with the respective heating rates of 5 and 10 °C min^{-1}, is clearly evidenced by the appearance of a strong peak at −34.6 ppm with multiples of spinning sidebands. This −34.6 ppm peak has been

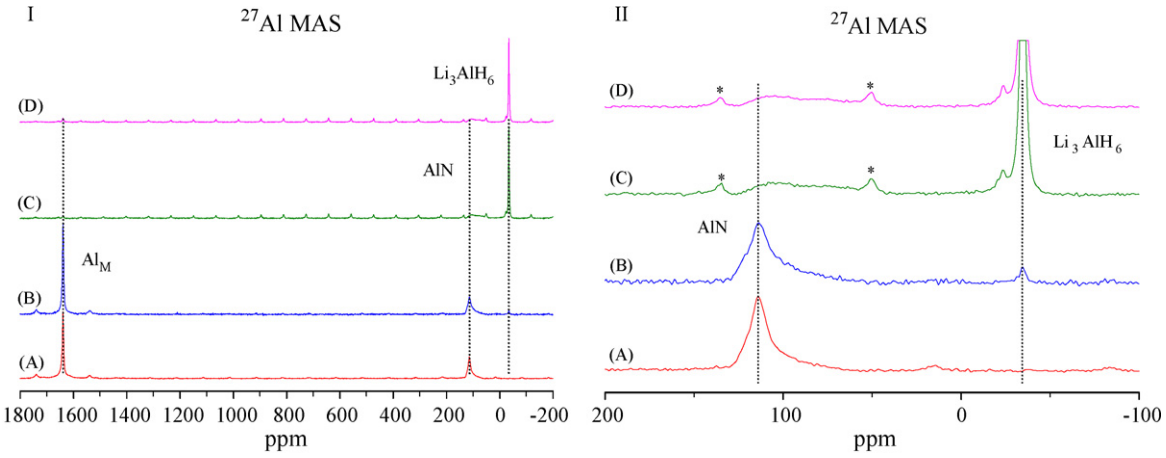

Fig. 4. ^{27}Al MAS NMR spectra of $3Li_2NH/Al/4$ wt%$TiCl_3$ after hydrogenation at 300 °C under 172 bar hydrogen pressure under the different heating rates: (A) 1 °C min^{-1}; (B) 2 °C min^{-1}; (C) 5 °C min^{-1} and (D) 10 °C min^{-1}. II are the expanded spectra between −100 ppm and 200 ppm. Peaks marked by * are spinning sidebands.

assigned to the Li_3AlH_6 phase [18,19]. The presence of Al metal in Sample 3 and 4 is negligible.

The population ratio similarly estimated by integrating the NMR peaks was Li_3AlH_6:Al_M:[AlN or Al_O (oxide phase)] = 74:1:25 for both Samples 3 and 4. It can be seen that the conversion of metallic Al to hexahydroaluminate (AlH_6^{3-}) was about 74%. At this point, the formation of AlN phase or other nitride species [16] can not be ruled out for these two samples. In any case, it is still valid to conclude that most Al_M converts into Li_3AlH_6 when the heating rate is $\geq 5\,^{\circ}C\,min^{-1}$.

The presence of Al_O detected for some samples by ^{27}Al NMR is also reported in reactive alanates such as the studies of Andrei et al. [20,21], in which aluminum oxide was detected by EELS during their experiments on $LiAlH_4$, even though the samples have been carefully transferred from the glove box to the instrument in a special vacuum transfer device including a removable glove bag mounted on the instrument.

Fig. 5 shows the ^6Li NMR spectra for the Samples 1–4, along with spectra of reference materials Li_2NH, $LiNH_2$, and LiH. The ^6Li MAS NMR shows superior resolution, in comparison to its ^7Li MAS NMR, for differentiating local environments of Li ions [22]. ^6Li MAS NMR spectra clearly reveal the transformation around amide/imide phases. Both Samples 3 and 4 show the characteristic three peaks at around 1.8 ppm in ^6Li NMR spectra (Fig. 5) which originate from three lithium sites [23] in $LiNH_2$. A ^6Li NMR reference spectrum from a mixed $LiNH_2$ + LiH sample is also provided at the bottom in Fig. 5. The single resonance at −0.9 ppm seen for both Samples 3 and 4 in Fig. 5C and D, respectively, can be assigned to Li_3AlH_6, which is an additional evidence for the re-formation of Li_3AlH_6 when the heating rates are 5 and $10\,^{\circ}C\,min^{-1}$. The LiH formation was not observed by ^6Li MAS NMR for these samples. As expected, ^6Li MAS NMR also reconfirms the absence of the Li_3AlH_6 formation in Sample 1 and 2 (heating rates are 1 and $2\,^{\circ}C\,min^{-1}$). The formation of LiH is clearly noticed by a peak at ∼0 ppm in Sample 1 while its formation could not be supported for Sample 2 by both ^6Li MAS and CPMAS (not shown) experiments. For the Samples 1 and 2, the formation of $LiNH_2$ seemed to be occurred while the ^6Li MAS NMR signature was not as clear as in samples with higher heating rates. It is interesting to note that the Sample 1 showed only two peaks out of the three peaks of $LiNH_2$. We currently do not have a reasonable interpretation on this observation except a speculation of excessive disorder among these sites obscuring resolution and relative intensities.

Table 1 summarizes the phases derived from XRD and NMR analyses. Based on all these results, it can be concluded that there are competing reactions during the hydrogenation process of Li_2NH + Al mixtures. The actual reactions that proceed and the reaction products depend strongly on the heating rate at which the samples are heated to the target reaction temperature. The formation of Li_3AlH_6 is achieved when heating rates $\geq 5\,^{\circ}C\,min^{-1}$ are employed. However, if slower heating rates are used, the formation of alternative nitride species appears to be preferred.

4. Summary

The effect of heating rate on the hydrogenation reactions of the mixture of $3Li_2NH$/Al/4 wt%$TiCl_3$ was investigated. The hydrogenated products were characterized by TGA, XRD and solid-state NMR. The results showed that the mixture can be hydrogenated, resulting in Li_3AlH_6 formation, under 172 bar hydrogen pressure and 300 °C with a heating rate faster than $5\,^{\circ}C\,min^{-1}$. Only partial hydrogenation ($Li_2NH \leftrightarrow LiNH_2 + LiH$) is achieved when the heating rate is slower than $2\,^{\circ}C\,min^{-1}$. The formation of the Li_3AlH_6 phase dominates when faster heating rates are used, while the formation of nitride species occurs when slow heating rates were used. The concerted effects of heating rate, temperature and hydrogen pressure have yet to be investigated thoroughly. To our best knowledge, we believe that we have identified for the first time the heating rate to be a crucial factor that has to be optimized for a reversible hydrogen storage system, at least for the $3Li_2NH$/Al/4 wt%$TiCl_3$ system studied here. Once aluminum nitride compounds get formed due to use of improper heating rates, the reversibility would be terminated.

Acknowledgement

This research was supported by the U. S. Department of Energy (DOE) under contract numbers DE-FC36-05GO15069 (U. Utah) and DE-AI-01-06EE11105 (JPL) and was also partially performed at the Jet Propulsion Laboratory, California Institute of Technology, under a contract with the National Aeronautical and Space Administration (NASA). The NMR facility at Caltech was supported by the National Science Foundation (NSF) under Grant Number 9724240 and partially supported by the MRSEC Program of the NSF under award number DMR-0520565. We thank W. Luo and J. W. Reiter for providing several Li–Mg–N–H reference materials.

References

[1] J. Chen, N. Kuriyama, Q. Xu, H.T. Takeshita, T. Sakai, J. Phys. Chem. B 105 (2001) 11214.
[2] J. Wang, A.D. Ebner, J.A. Ritter, J. Am. Chem. Soc. 128 (2006) 5949.
[3] A. Andreasen, T. Vegge, A.S. Pedersen, J. Solid State Chem. 178 (2005) 3672.
[4] O.M. Lovvik, S.M. Opalka, H.W. Brinks, B.C. Hauback, Phys. Rev. B 69 (2004) 134117.
[5] D. Blanchard, H.W. Brinks, B.C. Hauback, P. Norby, Mater. Sci. Eng. B 108 (2004) 54.
[6] V.P. Balema, V.K. Pecharsky, K.W. Dennis, J. Alloys Compd. 313 (2000) 69.
[7] V.P. Balema, J.W. Wiench, K.W. Dennis, M. Pruski, V.K. Pecharsky, J. Alloys Compd. 329 (2001) 108.
[8] A. Andreasen, J. Alloys Compd. 419 (2006) 40.
[9] J.H. Shim, G.J. Lee, Y.W. Cho, J. Alloys Compd. 419 (2006) 176.
[10] V.P. Balema, L. Balema, Phys. Chem. Chem. Phys. 7 (2005) 1310.
[11] W. Grochala, P. Edwards, Chem. Rev. 104 (2004) 1283.
[12] J.W. Jang, J.H. Shim, Y.W. Cho, B.J. Lee, J. Alloys Compd. 420 (2006) 286.
[13] J. Lu, Z.Z. Fang, J. Phys. Chem. B 109 (2005) 20830.
[14] J. Lu, Z.Z. Fang, H.Y. Sohn, J. Phys. Chem. B 110 (2006) 14236.
[15] Y. Kojima, M. Matsumoto, Y. Kawai, T. Haga, N. Ohba, K. Miwa, S.-I. Towata, Y. Nakamori, S.-I. Orimo, J. Phys. Chem. B 110 (2006) 9632.
[16] Z. Xiong, G. Wu, J. Hu, Y. Liu, P. Chen, W. Luo, J. Wang, Adv. Funct. Mater. 17 (2007) 1137.
[17] A.E. Bennett, C.M. Rienstra, M. Auger, K.V. Lakshmi, R.G. Griffin, J. Chem. Phys. 103 (1995) 6951.
[18] O. Dolotko, H. Zhang, O. Ugurlu, J.W. Wiench, M. Pruski, S.L. Chumbley, V. Pecharsky, Acta Mater. 55 (2007) 3121.
[19] J.W. Wiench, V.P. Balema, V.K. Pecharsky, M. Pruski, J. Solid State Chem. 177 (2004) 648.
[20] C.M. Andrei, J.C. Walmsley, H.W. Brinks, R. Holmestad, B.C. Blanchard, D. Hauback, G.A. Botton, J. Phys. Chem. B 109 (2004) 4350.
[21] M.H. Sørby, Y. Nakamura, H.W. Brinks, T. Ichikawa, S. Hino, H. Fujii, B.C. Hauback, J. Alloys. Compd. 428 (2007) 297.
[22] C.P. Grey, Y.J. Lee, Solid State Sci. 5 (2003) 883.
[23] R.C. Bowman Jr., J.W. Reiter, S.-J. Hwang, C. Kim, H. Kabbour, Proc. Int. Symp. Materials Issues Hydrogen Economy, Richmond, VA, November 12–15, 2007, in press.